Article

Discovery Medicine 2024; 36(183): 778–787
https://doi.org/10.24976/Discov.Med.202436183.73

Tropomyosin 2 Regulates Tumor Cell Proliferation, Immune Suppression, and Activation of the JNK Signaling Pathway in Colitis-Associated Cancer (CAC)

Aixi Sun[1,*], Jian Ge[2], Kaixin Ding[1], Zhiyang Gao[1], Yun Zhang[1]

[1]Department of Gastroenterology, Jinan Maternity and Child Care Hospital Affiliated to Shandong First Medical University Gastroenterology, 250218 Jinan, Shandong, China
[2]Department of Gastroenterology, Shandong Provincial Hospital Affiliated to Shandong First Medical University, 250021 Jinan, Shandong, China
*Correspondence: 19861855576@163.com (Aixi Sun)
Published: 20 April 2024

Background: Tropomyosin 2 (TPM2) has been linked to the advancement of various tumor types, exhibiting distinct impacts on tumor progression. In our investigation, the primary objective was to identify the potential involvement of TPM2 in the development of colitis-associated cancer (CAC) using a mice model.

Methods: This study used lentiviral vector complex for *TPM2* knockdown (*sh-TPM2*) and the corresponding negative control lentiviral vector complex (sh-NC) for genetic interference in mice. CAC was induced in mice using azoxymethane (AOM) and dextran sulfate sodium salt (DSS). This study included 6 groups of mice models: Control, Control+sh-NC, Control+sh-TPM2, CAC, CAC+sh-NC, and CAC+sh-TPM2. Subsequently, colon tissues were collected and assessed using quantitative reverse transcription-polymerase chain reaction (qRT-PCR) for *TPM2* mRNA levels and flow cytometry for infiltrating immune cells. Tumor number, size, and weight within colon tissues from CAC mice were measured and recorded. The hematoxylin-eosin staining was used for observing tissue pathology changes. The intestinal epithelial cells (IECs) were isolated and analyzed for cell proliferation. This analysis included examining the levels of 5-bromo-2-deoxyuridine (BrdU) and Ki-67 using immunohistochemistry. Additionally, the mRNA levels of proliferating cell nuclear antigen (PCNA) and Ki-67 were detected by qRT-PCR. This study also investigated the activation of the c-Jun N-terminal kinase (JNK) pathway using western blot analysis. Immunogenicity analyses were conducted using immunohistochemistry for F4/80 and flow cytometry.

Results: In 8-week-old mice, AOM injections and three cycles of DSS treatment induced TPM2 upregulation in tumor tissues compared to normal tissues ($p < 0.05$). Fluorescence-activated cell sorting (FACS)-isolated lamina CAC adenomas revealed macrophages and dendritic cells as primary TPM2 contributors ($p < 0.001$). Lentiviral *TPM2* gene knockdown significantly reduced tumor numbers and sizes in CAC mice ($p < 0.01$, and $p < 0.001$), without invasive cancer cells. TPM2 suppression resulted in decreased IEC proliferation ($p < 0.001$) and reduced PCNA and Ki-67 expression ($p < 0.05$). Western blot analysis indicated reduced JNK pathway activation in *TPM2*-knockdown CAC mice ($p < 0.05$, $p < 0.001$). *TPM2* knockdown decreased tumor-associated macrophage infiltration ($p < 0.01$) and increased CD3+ and CD8+ T cells ($p < 0.01$, and $p < 0.001$), with increased levels of regulator of inflammatory cytokines (CD44+, CD107a+) ($p < 0.01$, and $p < 0.001$), decreased levels of PD-1+ and anti-inflammatory factor (IL10+) ($p < 0.01$, and $p < 0.001$).

Conclusions: Our results demonstrated that *TPM2* knockdown suppressed the proliferation of CAC IECs, enhanced immune suppression on CAC IECs, and inhibited the JNK signaling pathway within the framework of CAC. These findings suggest TPM2 can serve as a potential therapeutic target for CAC treatment.

Keywords: tropomyosin 2; colitis-associated cancer; proliferation; immunosuppression; JNK signal pathway

Introduction

Chronic inflammation is often triggered by sustained and unregulated stimulation, often stemming from uncontrolled infections. This persistent activation not only perpetually stimulates epithelial cells but also promotes immune cell infiltration and the release of soluble mediators into the affected tissue. These circumstances can create an optimal microenvironment conducive to the development and progression of tumors [1]. Currently, chronic inflammation is identified as a fundamental element in cancer pathogenesis [2]. Ulcerative colitis (UC) is a specific subtype of inflammatory bowel disease (IBD), a group of disorders characterized by sustained and unexplained inflammation within the mucosal lining of the colon [3]. This chronic inflammatory condition affects the colon's mucosa, leading to a range of symptoms and complications. UC is considered an idiopathic disease, meaning its exact cause is not fully understood, making management challenging

and complex. IBD exemplifies the connection between persistent inflammation and cancer. Specifically, prolonged colon inflammation significantly increases the likelihood of developing colorectal cancer in the case of UC [4]. Colitis-associated cancer (CAC) is a primary contributor to mortality in individuals suffering from UC [5,6]. Although ongoing research investigates the cellular and molecular mechanisms connecting chronic inflammation to tumor development, our understanding of these mechanisms remains largely incomplete.

The tropomyosin 2 (*TPM2*) gene is recognized for its involvement in various rare myopathies [7]. Tropomyosin is essential for regulating muscle contraction through its interaction with the actin and troponin complexes. Simultaneously, it is vital for maintaining actin stability and contributes to cellular processes like cell migration. Recent research suggests a potential involvement of *TPM2* in cancer initiation [7]. Earlier studies have shown increased *TPM2* expression in early-stage colorectal cancers, indicating its possible involvement in colorectal adenoma progression [8,9]. Comparable experimental findings were verified in the context of hepatocellular carcinoma, indicating a noteworthy down-regulation of *TPM2* [10]. Furthermore, the absence of *TPM2* is linked to the unfavorable progression of prostate cancer [11]. However, the specific contribution of TPM2 to CAC development remains uncertain.

In this study, we investigated the significance of *TPM2* in the CAC tumorigenesis process. This investigation sought to determine whether TPM2-driven c-Jun N-terminal kinase (JNK) signaling contributes to the expedited growth of intestinal epithelial cells (IECs) and the immunosuppression associated with acute colitis.

Materials and Methods

Mice and CAC Model

We acquired 60 mice (C57BL/6, 30 ± 2 g, aged between 8–10 weeks) from the Chinese Academy of Sciences. The lentivirus transfection complex for *TPM2* knockdown (*sh-TPM2*; GCAGAGTATGTCACTATTTCC) and its lentiviral negative control complex (sh-NC; UUCUCCGAACGUGUCACGUTT) were obtained from GeneChem (Shanghai, China). The colon carcinogen azoxymethane (AOM; HY-111379, MedChemExpress, Monmouth Junction, NJ, USA) was used to induce colon cancer while dextran sulfate sodium salt (DSS; 160110, MP Biomedicals (Shanghai) Co., Ltd., Shanghai, China) was used to induce colitis. Mice were randomized into six groups (Control group, Control+sh-NC group, Control+sh-TPM2 group, CAC group, CAC+sh-NC group, CAC+sh-TPM2 group), with 10 mice in each group. Ethical approval was granted by the Ethics Committee of Jinan Maternity and Child Care Hospital Affiliated to Shandong First Medical University (No. 078 in 2022 for Animal Ethics Approval). The establishment of mouse CAC models in this study followed previously developed protocols [12]. In the Control group, the mice were kept under normal conditions without drug intervention. In the Control+sh-NC/sh-TPM2 group, sh-NC/sh-TPM2 were intraperitoneally injected into the normal-kept mice. In the CAC group, the mice received intraperitoneal injections of AOM at 15 mg/kg body weight. Following a 5-day interval, they were administered drinking water with 2.5% DSS (w/v) for five days. In the CAC+sh-NC/sh-TPM2 groups, sh-NC/sh-TPM2 was intraperitoneally injected into the mice based on the CAC model. The basis of a successful mice CAC model involves firstly inducing associated carcinogenesis through AOM treatment and subsequent induction of chronic colitis through DSS treatment. Colitis or CAC models were successfully established in all mice. Following the initial 5-day treatment period, the mice were transitioned back to regular drinking water for the following 15 days. This phase of the experiment was then succeeded by the introduction of two more DSS treatment cycles, as illustrated in Fig. 1A. On the 100th day, mice were euthanized by intraperitoneal injection of pentobarbital sodium (3 g/100 mL) (120 mg/kg), followed by removal of the distal colons (terminal 2.5 cm). After colons were rinsed with phosphate-buffered saline (PBS; C0221A, Beyotime, Shanghai, China), the tumors count, weight, and diameter were measured and recorded. Afterward, pathological tissues were promptly frozen at –80 °C to be prepared for histological analysis.

Hematoxylin-Eosin (H&E) Staining

The frozen colon tissues were placed in 4% paraformaldehyde (P0099, Beyotime, Shanghai, China) overnight and were then embedded in paraffin and cut into 7-µm sections. The histological examination involved various immunohistochemical staining techniques, including hematoxylin-eosin staining by the assay kit (C0105S, Beyotime, Shanghai, China). This process involved immersing sections in hematoxylin solution, followed by eosin staining, and subsequent observation through an optical microscope (CX31, Olympus, Tokyo, Japan).

Immunohistochemistry

The paraffin-embedded tissue sections were deparaffinized. After sections were treated with antigen retrieval solution (P0090, Beyotime, Shanghai, China), they were incubated with 0.3% H_2O_2 (P0100, Beyotime, Shanghai, China) and normal goat serum (C0265, Beyotime, Shanghai, China) to block nonspecific binding. After washing with PBS, sections were incubated overnight at 4 °C with primary antibodies of anti-F4/80 (1:200, PA1046, Biossci, Wuhan, China), anti-5-bromo-2-deoxyuridine (BrdU; 1:200, ab152095, Abcam, Cambridge, MA, USA), and anti-Ki-67 (1:100, PA1007, Biossci, Wuhan, China). Following incubation, peroxidase staining was conducted using the Streptavidin-Peroxidase Kit (A0305, Beyotime, Shanghai, China) and detected the target proteins with 3,3′-

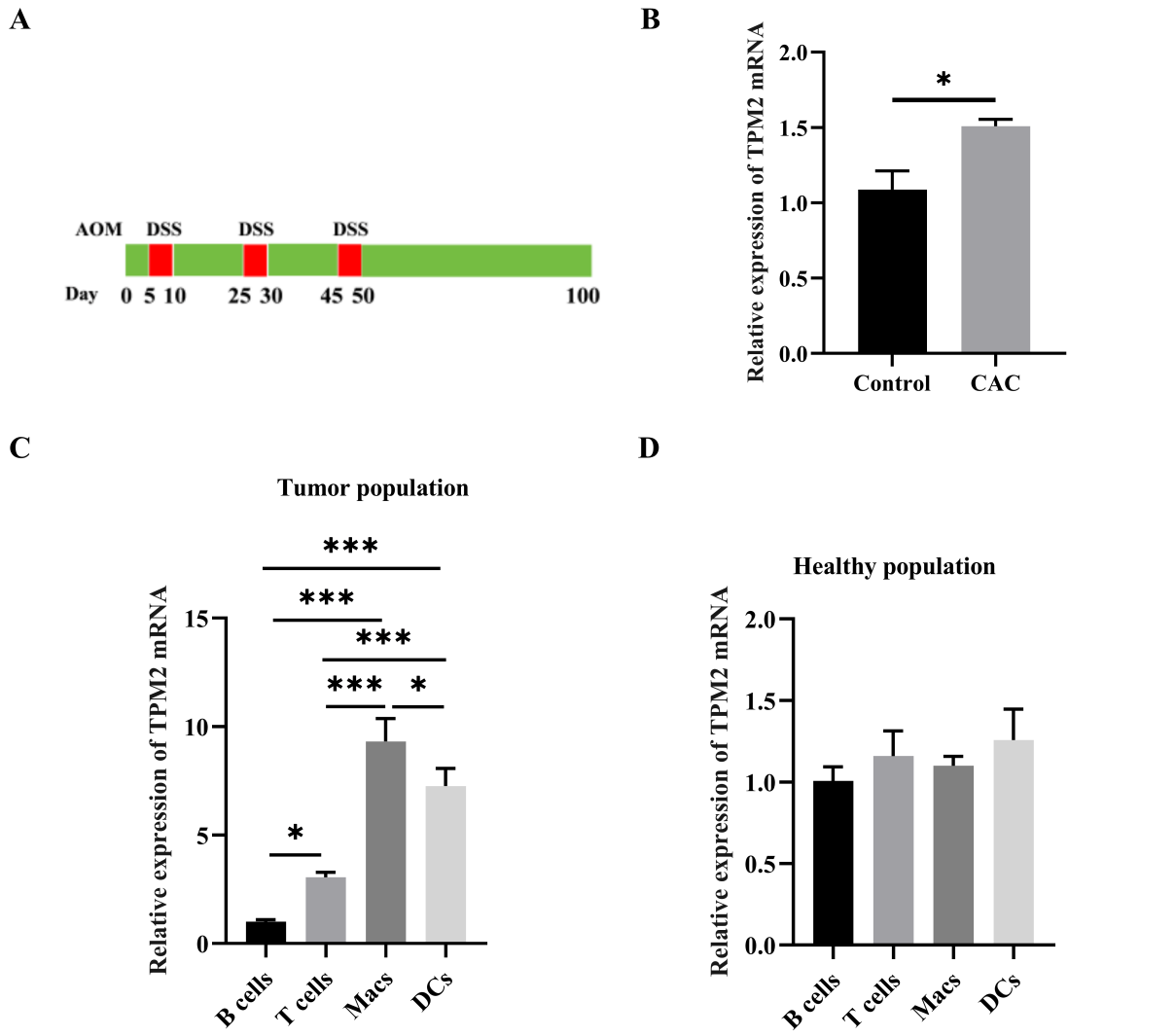

Fig. 1. Tropomyosin 2 (TPM2) expression exhibited an increase in colitis-associated cancer (CAC). (A) The model scheme of the CAC. (B) Quantitative real-time polymerase chain reaction (qRT-PCR) was employed to evaluate TPM2 expression in colon tissues obtained from mice in the Control and CAC groups. (C,D) The mRNA levels of *TPM2* were scrutinized using qRT-PCR within T cells, B cells, macrophages, and dendritic cells isolated from activated cells through fluorescence-based methods. Tumor population refers to the cells infiltrating the tumors from CAC mice models in CAC group, whereas the healthy population refers to cells obtained from the colon tissues in healthy, disease-free mice from Control group. n = 10, *$p < 0.05$, ***$p < 0.001$. AOM, azoxymethane; DSS, dextran sulfate sodium salt; Macs, Macrophages; DCs, Dendritic Cells.

diaminobenzidine (HY-15912, MedChemExpress, Monmouth Junction, NJ, USA). All samples were visualized using a light microscope (CX31, Olympus, Tokyo, Japan) and quantitative analysis was conducted using ImageJ software (version 1.5f, National Institutes of Health, Rockville, MD, USA).

Quantitative Real-Time Polymerase Chain Reaction (qRT-PCR)

We initiated our study by extracting total RNA from the samples using the TRIzol Universal reagent (R0016, Beyotime, Shanghai, China). Subsequently, we employed the cDNA first strand synthesis kit (D7168, Beyotime, Shanghai, China) and SuperReal fluorescence quantitative premix reagent (FP206, Tiangen, Beijing, China) to eliminate genomic DNA and synthesize complementary DNA. The PikoRealTM Real-Time PCR system (Roche, Basel, Switzerland) was utilized to assess the mRNA expression levels, running all sample primers in triplicate for robust results. Relative quantitative analysis relied on the $2^{-\Delta\Delta Ct}$ method, with GAPDH serving as the internal reference for data standardization. This comprehensive approach allowed ensured the accurate evaluation of the mRNA expression efficiency in our samples. The sequences employed in this research are detailed in Table 1.

Table 1. The primer sequences employed in this research.

Primer names	Primer sequence (5′-3′)
TPM2-F	GGTGGCCGAGAGTAAATGTGG
TPM2-R	TTTGGTGGAATACTTGTCCGC
PCNA-F	TGTTGGAGGCACTCAAGGAC
PCNA-R	AACTTTCTCCTGGTTTGGTGC
Ki-67-F	GCAAGAGGCAGCAAAGGTC
Ki-67-R	ATTGTCCACTGTCACTGAATCC
GAPDH-F	AACGACCCCTTCATTGAC
GAPDH-R	TCCACGACATACTCAGCAC

TPM2, tropomyosin 2; PCNA, proliferating cell nuclear antigen; F, forward; R, reverse.

Western Blot

The protein isolation process was executed using SDS-polyacrylamide gel (P0937, Beyotime, Shanghai, China) electrophoresis, followed by transfer onto a polyvinylidene fluoride (PVDF) membrane (FFP22, Beyotime, Shanghai, China). To facilitate antibody binding, a 5% BSA solution (ST025, Beyotime, Shanghai, China) was applied to the PVDF membrane at 25 °C for 1 hour. Antibodies specific to JNK (1:2000 dilution; cat no. 66210-1-Ig, Proteintech, Wuhan, China), and c-Jun (1:1000 dilution; cat no. ab40766, Abcam, Cambridge, MA, USA), phosphorylated (p)-c-Jun (1:1000 dilution; cat no. ab81319, Abcam, Cambridge, MA, USA), and p-JNK (1:1000 dilution; cat no. ab215208, Abcam, Cambridge, MA, USA), and GAPDH (1:1000 dilution; cat no. ab9485, Abcam, Cambridge, MA, USA) were then applied and left to incubate on the membranes at 4 °C for 12 hours. The PVDF membrane, along with the primary antibody complex, was further treated with a secondary antibody at a 1:2000 dilution (cat no. ZB-2305/ZB-2301, ZSGB-BIO, Beijing, China). Protein detection used a chemiluminescence enhancement kit (P0018S, Beyotime, Shanghai, China), and grayscale values were measured using ImageJ software (version 1.5f, National Institutes of Health, Rockville, MD, USA).

Cell Harvest and Flow Cytometry

Tissue was thoroughly washed with PBS, finely minced, and enzymatically digested using collagenase I and DNase I (B20223, Sigma-Aldrich, Saint Louis, MO, USA) for 30 minutes at 37 °C. Following centrifugation, the cell suspension was collected and re-suspended in F12 medium (iCell-0006, Bioscience, Shanghai, China). CD16/CD32 monoclonal antibody (56-0161-82, Invitrogen, Carlsbad, CA, USA) was then introduced into the cell suspension to facilitate immunophenotyping. The isolated cells were then incubated with mouse-specific fluorescent markers, CD3 (14-0037-82, Invitrogen, Carlsbad, CA, USA), CD8 (11-0081-82, Invitrogen, Carlsbad, CA, USA), interleukin-10 (IL-10; 17-7101-82, Invitrogen, Carlsbad, CA, USA), programmed cell death protein 1 (PD-1; 11-9985-82, Invitrogen, Carlsbad, CA, USA), CD44 (12-0441-82, Invitrogen, Carlsbad, CA, USA), and CD107a (53-1071-82, Invitrogen, Carlsbad, CA, USA). Intracellular cytokine staining was conducted using the Fixation/Permeabilization Solution Kit (554715, BD Biosciences, San Jose, CA, USA) and flow cytometry analyses were performed with a flow cytometer (LSRFortessa™, BD Biosciences, San Jose, CA, USA), enabling comprehensive characterization and assessment of immune cell populations within both tumor and colonic tissues in the mice. This approach provided valuable insights into the intricate immune responses and cellular dynamics within the experimental subjects.

Fluorescence-Activated Cell Sorting (FACS)

Cell suspension was prepared containing the intrinsic layer and CAC tumor cells. This process may involve tissue sample dissociation, preparation of single-cell suspensions, and cell culturing in an appropriate medium. Fluorescently labeled antibodies (CD19 antibodies (ab245235, Abcam, Cambridge, UK) label B cells, CD3 antibodies (ab16669, Abcam, Cambridge, UK) label T cells, CD68 antibodies (ab283654, Abcam, Cambridge, UK) label macrophages, and CD86 antibodies (ab239075, Abcam, Cambridge, UK) label dendritic cells) were added to the cell suspension to distinguish between intrinsic layer and CAC tumor cells, with each antibody associated with distinct fluorescent colors to differentiate them. Cells were incubated with the antibody mixture to ensure binding of the antibodies to the corresponding surface antigens on the cells. The post-incubation cell suspension was loaded into the FACS instrument for cell sorting (BD FACS Calibur, BD Biosciences, San Jose, CA, USA).

Isolation of Tumor Epithelial Cells

Tumor tissues were cut into approximately 1 mm pieces before being subjected to digestion with 12 mg/mL collagenase-DNase I (B20223, Sigma-Aldrich, Saint Louis, MO, USA) and straining through 100 and 70 µm cell strainers to obtain a cell suspension. The isolated cells were cultured on plates coated with 5 mg/mL rat tail collagen type I (C3867, Sigma-Aldrich, Saint Louis, MO, USA) in F12 medium (iCell-0006, Bioscience, Shanghai, China). We observed morphology of the isolated primary cells using a microscope (CX31, Olympus, Tokyo, Japan). Additionally, primary cells were labeled with an epidermal growth factor receptor (EGFR) antibody (MA-13319, Invitrogen, Carlsbad, CA, USA) according to the manufacturer's instruction, and detected by fluorescence microscopy (BX53, Olympus, Tokyo, Japan). Isolated cells were negative for mycoplasma. This comprehensive culture system provided the optimal conditions for the growth and maintenance of these colonic immune cells for subsequent analysis.

Statistical Analyses

The data were presented as mean values ± standard deviation. Significance was determined as $p <$

0.05. Statistical analysis was conducted using GraphPad Prism Software 8.0 (San Diego, CA, USA, available at https://www.graphpad-prism.cn/). The data were subjected to statistical analysis using *T*-tests and the analysis of variance (ANOVA; Tukey's post hoc analysis) to ascertain significant differences and trends.

Results

The Expression of TPM2 in CAC was Up-Regulated

Our hypothesis centered on the potential variation in TPM2 expression in AOM/DSS-induced tumors. In our study, 8-week-old mice were administered AOM injections and subjected to three cycles of DSS treatment, as depicted in Fig. 1A. Subsequently, we harvested tumor tissues from CAC model mice in the CAC group and normal tissues from healthy rats in the Control group for TPM2 expression evaluation via qRT-PCR. The results revealed a significant upregulation in TPM2 expression within tumor tissues compared to normal tissues, as depicted in Fig. 1B ($p < 0.05$). Subsequently, lamina CAC adenomas were isolated using fluorescence-activated cell sorting (FACS). The gene expression levels of *TPM2* were quantified in the sorted cells, demonstrating that macrophages and dendritic cells were the primary contributors to TPM2 production, with T cells closely following suit, as visualized in Fig. 1C ($p < 0.05$, $p < 0.01$, and $p < 0.001$). In Fig. 1D, TPM2 expression among various immune cells in the healthy population displayed no significant differences. This comprehensive analysis provides insights into the key contributors to TPM2 expression within the tumor microenvironment.

Deletion of TPM2 Reduced CAC Tumorigenesis

This study employed lentiviral transfection to suppress the *TPM2* gene in mice, aiming to assess the impact of *TPM2* knockdown on CAC sensitivity. *TPM2* gene knockdown efficiency was measured through qRT-PCR technology and shown in Fig. 2A. Compared to the CAC+sh-NC group, the *TPM2* mRNA levels were significantly reduced in the CAC+sh-TPM2 group ($p < 0.01$). Notably, we observed a substantial decrease in both the number (Fig. 2B; $p < 0.001$) and size (Fig. 2C; $p < 0.01$) of tumors in CAC mice with *TPM2* gene knockdown compared to the pure CAC model. This reduction in tumor weight was further illustrated in Fig. 2D ($p < 0.001$). Notably, invasive cancer cells were not detected in either the CAC+sh-NC or CAC+sh-TPM2 group, as illustrated in Fig. 2E. These results suggest that *TPM2* gene knockdown has a significant impact on tumor development, resulting in reduced tumor numbers and sizes, without evidence of invasive cancer cells in the studied models.

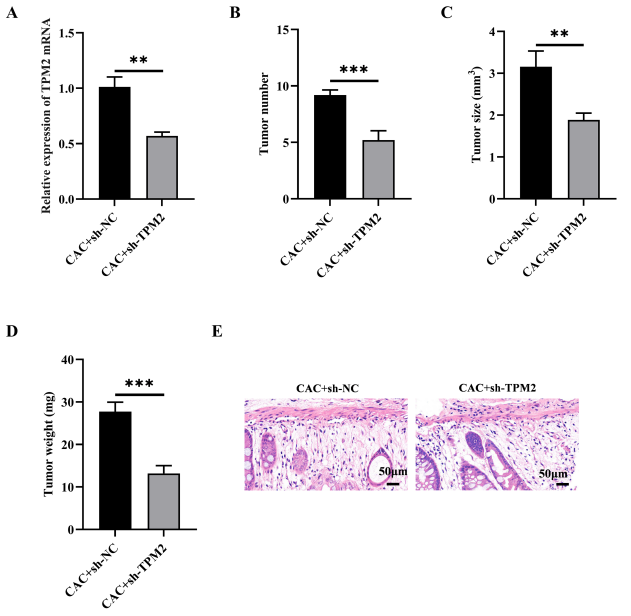

Fig. 2. Knockdown of *TPM2* exhibited an inhibitory effect on tumor development in CAC mouse models. (A–D) (A) The mRNA level of TPM2 determined by qRT-PCR. After 100 days of CAC induction, (B) the count of tumors, (C) tumor dimensions, and (D) tumor weight were measured. (E) Histological examination of colon tissues. Scale bar: 50 μm. n = 10, $^{**}p < 0.01$, $^{***}p < 0.001$. *sh-TPM2*, *TPM2* knockdown; sh-NC, negative control lentiviral vector complex.

TPM2 Knockdown Inhibited the CAC Tumor Cell Proliferation and Tumor Growth

To investigate the influence of TPM2 on the IEC proliferation in CAC tissues, we administered 5-bromo-2-deoxyuridine (BrdU) to both healthy mice in the Control group and CAC mice in the CAC group. The proliferation of IECs within the crypts of sh-TPM2-transfected CAC mice significantly decreased compared to sh-NC-transfected CAC mice, as indicated in Fig. 3A ($p < 0.001$). These findings were further substantiated by the expression of Ki-67 in the crypts (Fig. 3B; $p < 0.001$). Moreover, the proliferating cell nuclear antigen (PCNA) mRNA levels significantly decreased in tumor tissues from CAC mince transfected with sh-TPM2 (Fig. 3C; $p < 0.05$). Additionally, Ki-67 mRNA expression was significantly lower in sh-TPM2-transfected CAC tumor tissues compared to sh-NC-transfected CAC tumor tissues (Fig. 3D; $p < 0.01$). These results collectively demonstrate a substantial reduction in tumor growth capacity under the *TPM2* knockdown condition.

TPM2 Downregulation Inhibited JNK Signaling Activation in CAC

To better understand the molecular mechanisms underlying the role of TPM2 in mediating CAC tumor growth and proliferation, we conducted a western blot analysis us-

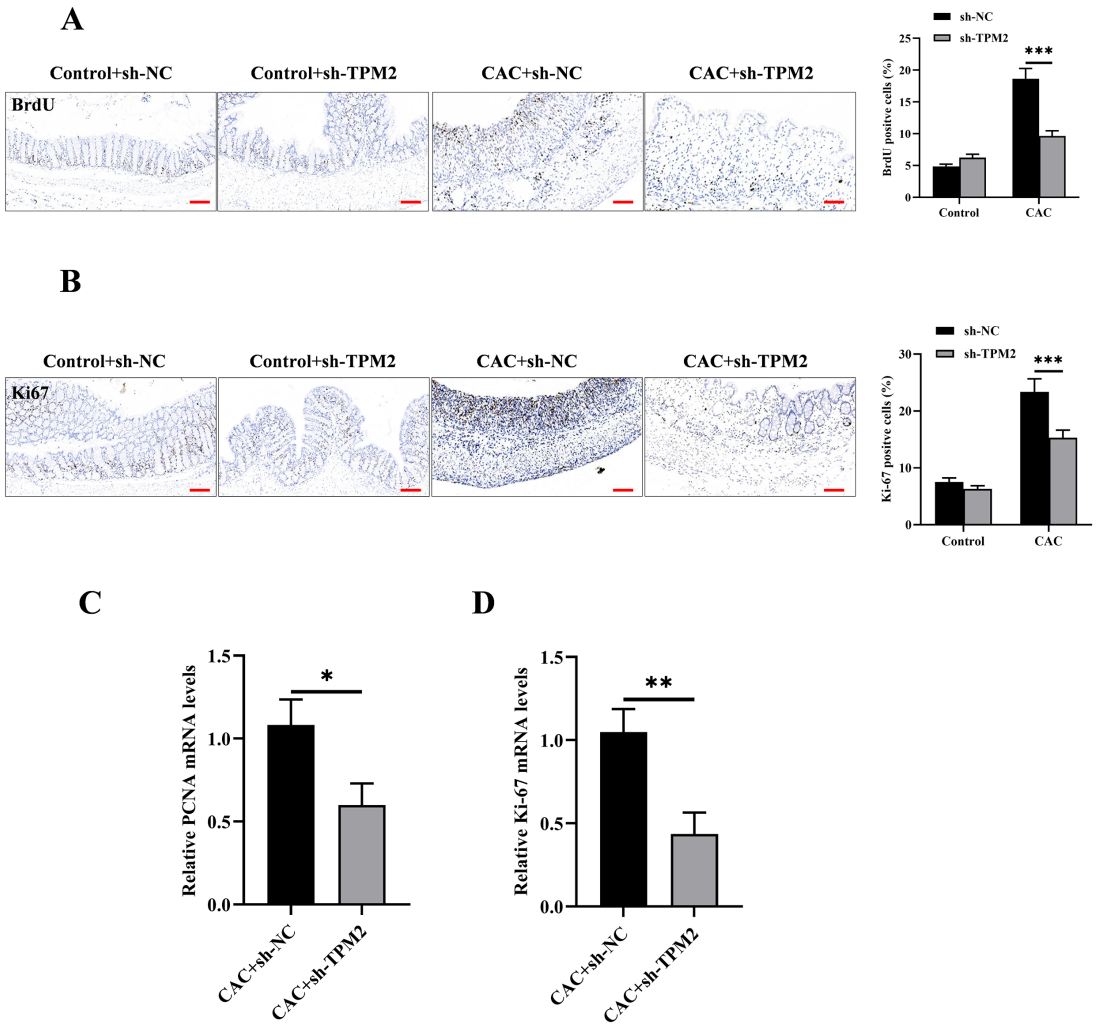

Fig. 3. *TPM2* knockdown inhibited CAC tumor cell proliferation and tumor growth. (A) The extent of proliferation of mid-gut epithelial cells in mice colon tissues determined by 5-bromo-2-deoxyuridine (BrdU) labeling and immunohistochemistry. Scale bar: 50 µm. (B) Proliferation determined by Ki-67 staining and the quantification of Ki-67-positive cells. Scale bar: 50 µm. (C,D) The mRNA expression levels of proliferating cell nuclear antigen (PCNA) and Ki-67 in CAC tumor tissues. n = 10, *$p < 0.05$, **$p < 0.01$, ***$p < 0.001$.

ing colonic lysates. The results of this analysis reveal a notable decrease in the phosphorylation of both JNK (p-JNK; $p < 0.01$) and its major substrate, c-JUN (p-c-JUN; $p < 0.01$), in CAC mice transfected with sh-TPM2 compared to CAC mice transfected with sh-NC (Fig. 4). This finding suggests that TPM2 plays a crucial role as a JNK pathway activator in CAC tumor growth.

TPM2 Knockdown Enhanced the Immunogenicity of Tumor Microenvironment (TME) during CAC

To investigate whether TPM2 is implicated in immune cell infiltration, this study analyzed immune cell profiles within the colonic mucosa of CAC mice. Notably, *TPM2* knockdown in CAC mice led to decreased infiltration of tumor-associated macrophages, as depicted in Fig. 5A ($p < 0.001$). Moreover, *TPM2*-knockdown CAC mice exhibited a significant increase in the number of CD3+ (Fig. 5B; $p < 0.01$) and CD8+ (Fig. 5C; $p < 0.001$) T cells within the tumor microenvironment. Additionally, *TPM2* knockdown in CAC mice corresponded with lower IL-10 (Fig. 5D; $p < 0.001$) and PD-1 (Fig. 5E; $p < 0.01$) expression levels, and higher CD44 (Fig. 5F; $p < 0.001$) and CD107a (Fig. 5G; $p < 0.001$) expression levels compared to CAC mice without genetic interference. These findings suggest that TPM2 plays a critical role in regulating immune cell infiltration and the associated cytokine expression within the tumor microenvironment.

Discussion

CAC represents the most severe complication arising from inflammatory bowel disease [13]. Initial investigations have indicated a significant association between

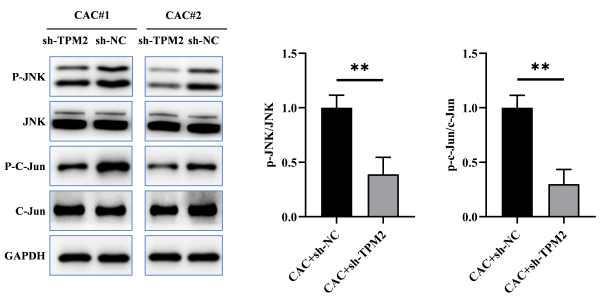

Fig. 4. TPM2 deletion resulted in the inhibition of c-Jun N-terminal kinase (JNK) signaling in CAC. Two representative images of western blot analysis and the corresponding quantification. n = 10, $^{**}p < 0.01$.

TPM2 and the unfavorable prognosis of colorectal cancer [14]. Prior research has established a strong link between TPM2 expression, the proliferation and migratory abilities of colorectal cancer cells [15]. Nonetheless, the precise function of TPM2 in governing the initiation and progression of CAC has yet to be elucidated. However, this study identifies that TPM2 exerts control over JNK signaling, proliferation of precancerous IECs, and the immune modulation within the tumor microenvironment during inflammation-related colon carcinogenesis. Consequently, targeting TPM2 signaling may offer an innovative therapeutic and preventative approach for addressing CAC.

Relevant research has indicated an increase in TPM2 expression in colorectal cancer [15]. Our findings clearly illustrate that TPM2 expression is elevated in colitis-associated tumors in mice. Remarkably, mice with *TPM2* knockdown displayed a reduction in both the number and size of adenomas compared to mice without TPM2 genetic interference.

Current research has revealed that TPM2 plays an essential role in the development of human primary colon cancer in the presence of intestinal inflammation [16]. Our data suggests that TPM2 downregulation notably decreased the proliferation of IECs isolated from colon tissues of CAC mice. Interestingly, it appears that the proliferation of IECs associated with tissue repair may also have implications on tumor growth. As a result, *TPM2* knockdown during CAC induction leads to a significant reduction in both tumor burden and growth, evident from the decreased expression of proliferation markers like PCNA and Ki-67. Thus, the observed decrease in IECs proliferation may help explain the heightened colitis and the reduced incidence of colorectal adenomas in TPM2-deficient mice. This intriguing finding highlights the complex interplay between TPM2, colitis, and the development of colorectal tumors in an inflammatory context.

The JNK pathway's involvement in oncogenic transformations and cell proliferation is well-documented across a diverse spectrum of cancer types [17,18]. This signaling pathway, which includes c-Jun N-terminal kinases (JNKs), plays a critical role in facilitating the uncontrolled growth of cancer cells and their transformation into malignant forms [19]. Its common presence in cancer tissues contributes to their aggressiveness and progression [20], making the JNK pathway a potential target for therapeutic interventions to curb tumor growth and metastasis. Understanding the JNK pathway's role in different cancer types is pivotal for the development of precise and effective treatment strategies. Liu *et al*. [12] documented the significance of the JNK pathway in the initiation and advancement of colon cancer. Their research shed light on the pivotal role played by the JNK pathway in the development and progression of this particular cancer type.

Activation of the JNK/c-Jun signaling pathway has been found to expedite the progression of colorectal tumorigenesis [21]. Conversely, inhibiting c-Jun activity decreases progenitor cell proliferation, thereby delaying the onset and development of tumors in mice. This highlights the critical role of JNK/c-Jun signaling in the modulation of colorectal cancer progression, presenting it as a potential target for therapeutic interventions. Yet, the existence of feedback regulation between TPM2 and the JNK pathway has remained a mystery. However, this study has unveiled that the TPM2 downregulation significantly decreases the expression levels of phosphorylated JNK (p-JNK) and phosphorylated c-Jun (p-c-Jun) in mouse models with colitis and CAC. This suggests a dynamic interplay between TPM2 and the JNK pathway, where TPM2 appears to influence the activation of the JNK signaling cascade, potentially unveiling a novel layer of regulatory complexity in these processes.

In the context of CAC, TPM2 deletion induces a transformation in the immunogenic phenotype. This transformation is characterized by an increase in tumor-infiltrating CD8+ T cells and concurrent reductions in myeloid-derived suppressor cells (MDSC) and tumor-associated macrophages (TAMs). Furthermore, TAMs exhibit a notable shift toward polarization into the M1 phenotype. These immune changes signify the intricate regulatory role of TPM2 in shaping the immune landscape within the tumor microenvironment during CAC.

The depletion of myeloid-derived suppressor cells (MDSC) and tumor-associated macrophages (TAMs) paves the way for the generation of immunophenotypic T cells, which exhibit potent and effective antitumor properties [22]. This process highlights the critical role of immune cell modulation in improving the body's defenses against cancer. The development of clinical therapeutic agents that target TPM2 signaling may revolutionize cancer therapy. As a result, the strategy of expanding and activating T cells by inhibiting TPM2 signaling holds promise as a pathway to heighten T cell activity and enhance immune effectiveness for cancer treatment.

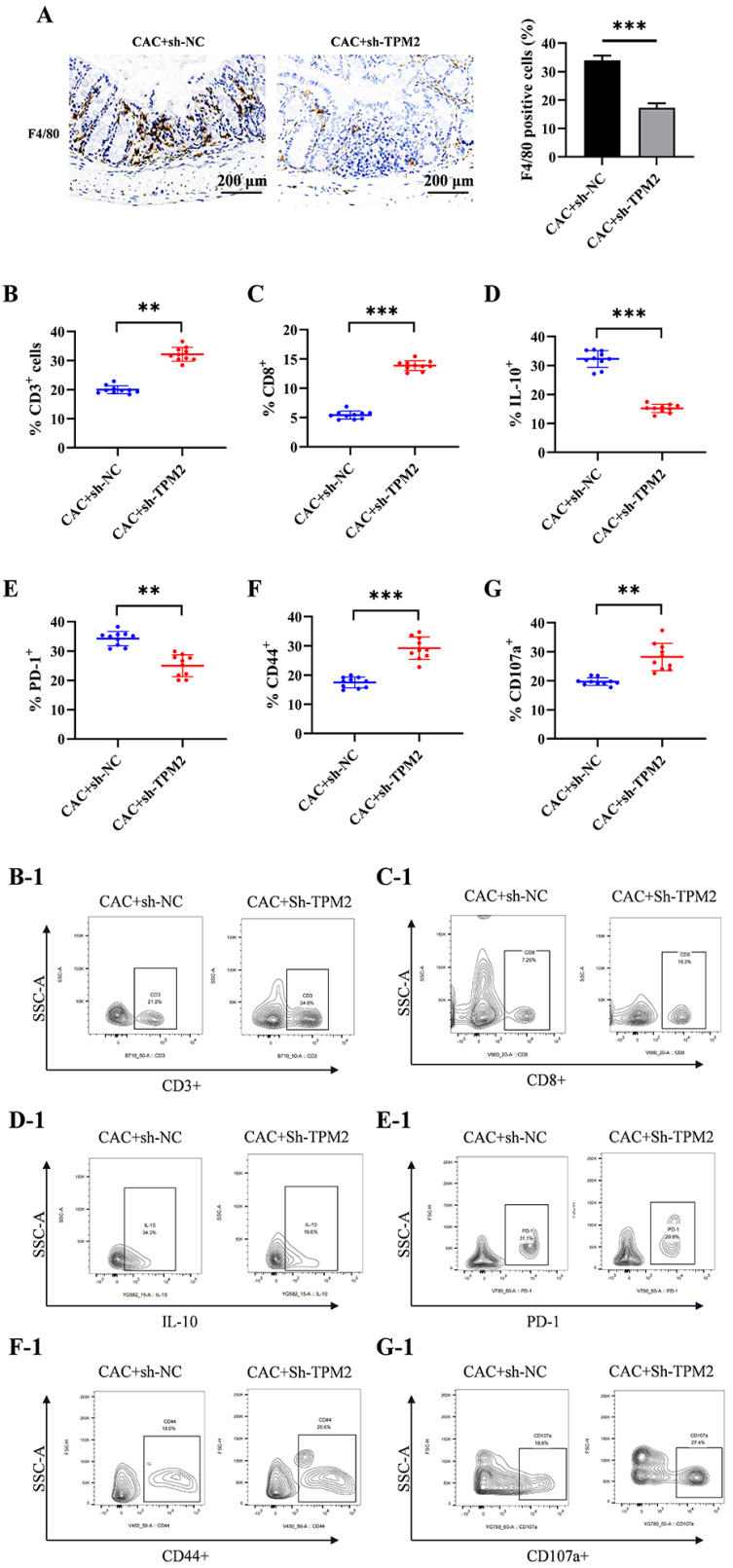

Fig. 5. The knockdown of *TPM2* amplified the immunogenic characteristics of the tumor microenvironment in CAC. (A) Immunohistochemistry analysis for F4/80 was conducted on colon tissues from mice with adenomas. (B&B-1,C&C-1) Flow cytometry was employed to calculate the proportions of CD3+ and CD8+T cells within the adenomas. (D&D-1, E&E-1, F&F-1, G&G-1) Flow cytometry was utilized to assess the expression levels of interleukin-10 (IL-10), programmed cell death protein 1 (PD-1), CD44, and CD107a in the adenoma mice. n = 10, $^{**}p < 0.01$, $^{***}p < 0.001$.

Conclusions

Our findings demonstrated the pivotal role of TPM2 in fostering the proliferation of IECs and enhancing the immunosuppressive effects on CAC IECs. These findings highlight the multifaceted involvement of TPM2 in both the early stages of CAC development and the complex interaction with immune responses, providing TPM2 as a potential therapeutic target for treating or ameliorating CAC.

Availability of Data and Materials

The datasets used and/or analyzed during the current study are available from the corresponding author on reasonable request.

Author Contributions

Provided the main idea for the research and designed the experimental plan: AS. Conducted experiments and collected data: JG. Assisted in designing the experimental plan: KD. Conducted experiments and collected data: ZG. Assisted in designing the experimental plan: YZ. All authors contributed to editorial changes in the manuscript. All authors read and approved the final manuscript. All authors have participated sufficiently in the work and agreed to be accountable for all aspects of the work.

Ethics Approval and Consent to Participate

Ethical approval was granted by the Ethics Committee of Jinan Maternity and Child Care Hospital Affiliated to Shandong First Medical University (No. 078 in 2022 for Animal Ethics Approval).

Acknowledgment

Not applicable.

Funding

This research received no external funding.

Conflict of Interest

The authors declare no conflict of interest.

References

[1] Afify SM, Hassan G, Seno A, Seno M. Cancer-inducing niche: the force of chronic inflammation. British Journal of Cancer. 2022; 127: 193–201.

[2] Sohrab SS, Raj R, Nagar A, Hawthorne S, Paiva-Santos AC, Kamal MA, *et al*. Chronic Inflammation's Transformation to Cancer: A Nanotherapeutic Paradigm. Molecules (Basel, Switzerland). 2023; 28: 4413.

[3] Seyedian SS, Nokhostin F, Malamir MD. A review of the diagnosis, prevention, and treatment methods of inflammatory bowel disease. Journal of Medicine and Life. 2019; 12: 113–122.

[4] Porter RJ, Kalla R, Ho GT. Ulcerative colitis: Recent advances in the understanding of disease pathogenesis. F1000Research. 2020; 9: F1000 Faculty Rev–294.

[5] Faye AS, Holmer AK, Axelrad JE. Cancer in Inflammatory Bowel Disease. Gastroenterology Clinics of North America. 2022; 51: 649–666.

[6] Thiele M, Donnelly SC, Mitchell RA. OxMIF: a druggable isoform of macrophage migration inhibitory factor in cancer and inflammatory diseases. Journal for Immunotherapy of Cancer. 2022; 10: e005475.

[7] Duan P, Cui J, Li H, Yuan L. Tropomyosin 2 exerts antitumor effects in lung adenocarcinoma and is a novel prognostic biomarker. Histology and Histopathology. 2023; 38: 669–680.

[8] Cui J, Cai Y, Hu Y, Huang Z, Luo Y, Kaz AM, *et al*. Epigenetic silencing of TPM2 contributes to colorectal cancer progression upon RhoA activation. Tumour Biology: the Journal of the International Society for Oncodevelopmental Biology and Medicine. 2016; 37: 12477–12483.

[9] Zhao B, Baloch Z, Ma Y, Wan Z, Huo Y, Li F, *et al*. Identification of Potential Key Genes and Pathways in Early-Onset Colorectal Cancer Through Bioinformatics Analysis. Cancer Control: Journal of the Moffitt Cancer Center. 2019; 26: 1073274819831260.

[10] Tian Z, Zhao J, Wang Y. The prognostic value of TPM1-4 in hepatocellular carcinoma. Cancer Medicine. 2022; 11: 433–446.

[11] Zhao HB, Xu GB, Yang WQ, Li XZ, Chen SX, Gan Y, *et al*. Bioinformatics-based identification of the key genes associated with prostate cancer. Zhonghua Nan Ke Xue = National Journal of Andrology. 2021; 27: 489–498.

[12] Liu ZY, Zheng M, Li YM, Fan XY, Wang JC, Li ZC, *et al*. RIP3 promotes colitis-associated colorectal cancer by controlling tumor cell proliferation and CXCL1-induced immune suppression. Theranostics. 2019; 9: 3659–3673.

[13] Shah SC, Itzkowitz SH. Colorectal Cancer in Inflammatory Bowel Disease: Mechanisms and Management. Gastroenterology. 2022; 162: 715–730.e3.

[14] Zhou Y, Bian S, Zhou X, Cui Y, Wang W, Wen L, *et al*. Single-Cell Multiomics Sequencing Reveals Prevalent Genomic Alterations in Tumor Stromal Cells of Human Colorectal Cancer. Cancer Cell. 2020; 38: 818–828.e5.

[15] Mele V, Basso C, Governa V, Glaus Garzon JF, Muraro MG, Däster S, *et al*. Identification of TPM2 and CNN1 as Novel Prognostic Markers in Functionally Characterized Human Colon Cancer-Associated Stromal Cells. Cancers. 2022; 14: 2024.

[16] Wang WJ, Li HT, Yu JP, Han XP, Xu ZP, Li YM, *et al*. A Competing Endogenous RNA Network Reveals Novel Potential lncRNA, miRNA, and mRNA Biomarkers in the Prognosis of Human Colon Adenocarcinoma. The Journal of Surgical Research. 2019; 235: 22–33.

[17] Kwak AW, Lee JY, Lee SO, Seo JH, Park JW, Choi YH, *et al*. Echinatin induces reactive oxygen species-mediated apoptosis via JNK/p38 MAPK signaling pathway in colorectal cancer cells. Phytotherapy Research: PTR. 2023; 37: 563–577.

[18] Kwak AW, Park JW, Lee SO, Lee JY, Seo JH, Yoon G, *et al*. Isolinderalactone sensitizes oxaliplatin-resistance colorectal cancer cells through JNK/p38 MAPK signaling pathways. Phytomedicine: International Journal of Phytotherapy and Phytopharmacology. 2022; 105: 154383.

[19] Oh BS, Im E, Lee HJ, Sim DY, Park JE, Park WY, *et al*. Inhibition of TMPRSS4 mediated epithelial-mesenchymal transition is critically involved in antimetastatic effect of melatonin in colorectal cancers. Phytotherapy Research: PTR. 2021; 35: 4538–4546.

[20] Tashireva L, Grigoryeva E, Alifanov V, Iamshchikov P, Zavyalova M, Perelmuter V. Spatial Heterogeneity of Integrins and Their Ligands in Primary Breast Tumors. Discovery Medicine. 2023; 35: 910–920.

[21] Wang H, Wen C, Chen S, Li W, Qin Q, He L, *et al*. ROS/JNK/C-Jun Pathway is Involved in Chaetocin Induced Colorectal Cancer Cells Apoptosis and Macrophage Phagocytosis Enhancement. Frontiers in Pharmacology. 2021; 12: 729367.

[22] Osipov A, Saung MT, Zheng L, Murphy AG. Small molecule immunomodulation: the tumor microenvironment and overcoming immune escape. Journal for Immunotherapy of Cancer. 2019; 7: 224.